

Research

Demographic and genetic collapses in spatially structured populations: insights from a long-term survey in wild fish metapopulations

Eglantine Mathieu-Bégné, Géraldine Loot, Mathieu Chevalier, Ivan Paz-Vinas and Simon Blanchet

E. Mathieu-Bégné (<https://orcid.org/0000-0002-6846-5491>) (eglantine.mb@gmail.com), *G. Loot*, *M. Chevalier* and *S. Blanchet*, Centre National de la Recherche Scientifique (CNRS), Univ. Paul Sabatier (UPS), Inst. de Recherche pour le Développement (IRD), Ecole Nationale Supérieure de Formation de l'Enseignement Agricole (ENSFEA); UMR5174, Evolution et Diversité Biologique, 118 route de Narbonne, FR-31062 Toulouse, France. LG also at: Inst. Universitaire de France, Paris, France. BS also at: CNRS, UPS; UMR5321, Station d'Ecologie Théorique et Expérimentale, Moulis, France. – *I. Paz-Vinas*, Univ. de Lyon, Ecole Nationale des Travaux Publics de l'Etat (ENTPE), CNRS; UMR5023, Laboratoire d'Ecologie des Hydrosystèmes Naturels et Anthropisés, Villeurbanne, France, and: UPS, INP, CNRS, Univ. de Toulouse, UMR 5245 Laboratoire Écologie Fonctionnelle et Environnement, Ecolab, Toulouse, France.

Oikos

00: 1–12, 2018

doi: 10.1111/oik-05511

Subject Editor: Florian Altermatt

Editor-in-Chief: Dries Bonte

Accepted 17 August 2018

Unraveling the relationship between demographic declines and genetic changes over time is of critical importance to predict the persistence of at-risk populations and to propose efficient conservation plans. This is particularly relevant in spatially structured populations (i.e. metapopulations) in which the spatial arrangement of local populations can modulate both demographic and genetic changes. We used ten-year demo-genetic monitoring to test 1) whether demographic declines were associated with genetic diversity declines and 2) whether the spatial structure of a metapopulation can weaken or reinforce these demographic and genetic temporal trends. We continuously surveyed, over time and across their entire range, two metapopulations of an endemic freshwater fish species *Leuciscus burdigalensis*: one metapopulation that had experienced a recent demographic decline and a second metapopulation that was stable over time. In the declining metapopulation, the number of alleles rapidly decreased, the inbreeding coefficient increased, and a genetic bottleneck emerged over time. In contrast, genetic indices were constant over time in the stable metapopulation. We further show that, in the declining metapopulation, demographic and genetic declines were not homogeneously distributed across the metapopulation. We notably identify one local population situated downstream as a 'reservoir' of individuals and genetic variability that dampens both the demographic and genetic declines measured at the metapopulation level. We demonstrate the usefulness of long-term monitoring that combines both genetic and demographic parameters to understand and predict temporal population fluctuations of at-risk species living in a metapopulation context.

Keywords: conservation genetics, rescue effect, fragmentation



Introduction

Understanding how demographic and genetic changes occur over time is critical to resolve evolutionary and conservation issues. Joint changes in demographic and genetic parameters over time have often been investigated through snap-shot approaches that investigate genetic changes between two (or more) periods during which demographic parameters have changed in the surveyed population (Schwartz et al. 2007, Habel et al. 2014). Nonetheless, using continuous monitoring (i.e. monitoring characterized by a regular temporal resolution) to conjointly study demographic and genetic changes over time should provide complementary information at a higher temporal resolution (Schwartz et al. 2007). For instance, demographic monitoring can provide information about the mechanisms responsible for temporal demographic changes (such as the intrinsic growth rate or density dependence, Hostetler and Chandler 2015), whereas genetic monitoring provides information regarding the evolutionary sustainability of populations (Schwartz et al. 2007). Thus, continuous real-time demo-genetic monitoring is a promising approach that should provide fundamental insights for the long-term conservation of populations (Hoban et al. 2014).

However, continuous real-time demo-genetic monitoring is still rarely used (but see Devillard et al. 2011, Chen et al. 2016). Most continuous real-time demo-genetic monitoring studies have focused on stable or increasing populations to assess their long-term genetic viability (Hansson et al. 2000, Kaeuffer et al. 2007, Devillard et al. 2011). Consequently, association between decreases in abundance (demographic collapses) and genetic diversity losses (genetic collapses) in declining populations has rarely been investigated in the wild. This is surprising given that association of demographic collapses and genetic diversity losses may sustain extinction vortices in at-risk populations. Particularly, Spielman et al. (2004) have shown that a loss in genetic diversity is expected to become critical before populations go extinct and this has consequences for the mechanisms that underline demographic changes (Cappuccino and Price 1995, Hildner et al. 2003). For instance, a loss in genetic diversity such as higher inbreeding depression in populations should decrease the intrinsic growth rate of these populations, hence favoring demographic declines (Cappuccino and Price 1995, Hostetler et al. 2013).

Association between demographic decline and loss of genetic diversity has been initially tested in populations homogeneously distributed in space (Spielman et al. 2004), but populations are often spatially structured across continuous or discontinuous habitat patches (Hanski 1998). This is the case for many natural ecosystems forming mosaics of habitats, such as rivers or oceans, but also for many ecosystems that are increasingly fragmented by human activities (e.g. through deforestation or the building of infrastructures). In these spatially structured landscapes, 'local' populations are connected to one another to form metapopulations, and some local populations may act as sources of individuals

and genes through emigration, whereas others may act as sinks, receiving individuals and genes through immigration (Gaggiotti 1996).

Predicting demo-genetic declines in metapopulations is not straightforward since both demographic changes and the distribution of genetic diversity are not necessarily spatially homogeneous (Naranjo and Bodmer 2007, Morrissey and de Kerckhove 2009). For instance, within a demographically declining metapopulation, if local source populations failed to provide enough individuals and genes to local sink populations, we can predict strong effects of genetic drift in local sink populations, but not necessarily in local source populations (Dunning et al. 1992, Spielman et al. 2004). As the population size decreases, the intensity of genetic drift increases in local sink populations, which may ultimately lead to local decreases in genetic diversity due to the loss or the fixation of particular alleles (Spielman et al. 2004, Potvin et al. 2017). In contrast, genetic rescue effects may be expected in local sink populations if they receive genetically distinct migrants from source populations (Dunning et al. 1992, Carlson et al. 2014). By dampening declines in genetic diversity through dispersal, local source populations may hence counteract the pervasive genetic consequences of demographic declines that occur at the metapopulation scale (Barson et al. 2009, Jangjoo et al. 2016). Testing whether demographic and genetic temporal changes are concomitant in declining metapopulations is consequently an important prerequisite to predict the sustainability of metapopulations in the long term (Vuilleumier et al. 2010, Palstra and Ruzzante 2011).

Here, we aimed to 1) test whether demographic declines over time are associated with changes in genetic diversity in the same timeframe in metapopulations and 2) identify to which extent the spatial structure of metapopulations may modulate these temporal trends. We focused on an endemic freshwater fish species from southwestern France (the rostrum dace, *Leuciscus burdigalensis*). We considered two metapopulations that belong to two sub-river basins that were surveyed demographically (by measuring local fish abundance) and genetically (by assessing genetic variation using neutral markers) for ten years on a year-to-year basis. One metapopulation underwent a sharp demographic decline during that period, whereas the other was stable (or slightly increased) demographically over time. We first quantified these demographic trends for both metapopulations and tested whether demographic changes were homogeneously distributed along the upstream–downstream gradients of the riverscapes. Second, we tested whether processes such as density-dependence and/or the effect of the intrinsic growth rates underlay these demographic changes. Then, we tested whether the general demographic decline observed in one of the two metapopulations was associated with a loss of genetic diversity over time. We further tested whether genetic diversity was homogeneously distributed along the upstream–downstream gradients of the riverscapes to identify the putative sources of genetic diversity. Finally, we evaluated the marginal impact of the spatial structure of the metapopulation on temporal genetic trends, notably by testing whether some local populations were

dampening genetic diversity losses occurring in other local populations by acting as reservoirs of individuals and genes.

According to Spielman et al. (2004), we predict a sharp and general decline in genetic diversity in the demographically collapsing metapopulation. Notably we expected an intrinsic negative growth rate underlying the demographic collapse and a departure from the Hardy–Weinberg equilibrium (which represents a genetic equilibrium expected in a stable population). However, riverscapes are strongly structured spatially and environmentally along the upstream–downstream gradient, which influences the demo-genetic dynamics of riverine metapopulations (Labonne et al. 2008, Altermatt 2013, Paz-Vinas and Blanchet 2015). Specifically, genetic diversity is generally higher in downstream local populations compared to upstream local populations in dendritic river networks (Paz-Vinas et al. 2015), and theory predicts that local extinction rates should be higher in local populations situated in isolated upstream localities (Gotelli and Taylor 1999, Mari et al. 2014). We can therefore expect that downstream localities will be 1) more demographically stable than upstream localities, and 2) potentially acting as reservoirs of genetic diversity, hence dampening (and potentially rescuing) the overall genetic consequences of the demographic decline (Fronhofer and Altermatt 2017).

Material and methods

Biological model and sampling design

Rostrum dace *Leuciscus burdigalensis* is a cyprinid species living in running waters with intermediate water temperature (from 14°C to 24°C in warmer months). It is a gregarious species living in small shoals of 3–5 individuals, and it generally feeds on benthic or drifting invertebrates. During the active season (June–October) dace forage in groups in habitats characterized by moderate to high water velocity (10–70 cm s⁻¹) and moderate water depth (20–60 cm depth), two characteristics that are generally not uniformly distributed across a whole stream. We can therefore consider that dace form metapopulations along the upstream–downstream gradient composed of discrete sub-populations (i.e. in habitats suitable for foraging) connected by corridors (i.e. unsuitable habitats for foraging). Dace can measure up to 30 cm in length, and can reach the age of 10–12 years. They are generally mature at ~2–3 years and they reproduce (several times along its lifetime) during spring on gravel beds of rivers, when the water temperature reaches ~9°C (Keith et al. 2011).

We sampled dace in the Viaur and Célé Rivers, two similar mid-size rivers (~150 km long) in the Garonne River Basin (southwestern France, Fig. 1). The Viaur and Célé Rivers are situated in two different sub-river basins (the Aveyron and Lot sub-river basins, respectively) separated from each other by more than 390 km of topological distance and by several impassable dams. Contemporary dispersal between the Viaur and Célé Rivers is hence highly unlikely (if not

impossible). Hence, we will hereafter consider that the local dace populations we sampled in these two rivers constitute two metapopulations whose contemporary dynamics are independent. Sampling was conducted yearly during the periods 2005–2014 and 2006–2014 for the Viaur and Célé Rivers, respectively, at eleven localities (i.e. river stretches of ~200 m long covering favourable foraging habitats for dace, Fig. 1). Sampled localities, which sustain local dace populations for each river, were separated by topological distance of at least 3.5 km that were often characterized by less favourable habitats (e.g. lentic river sections with low velocity and high water depth) that constitute dispersal corridors between two adjacent local dace populations. Sampling localities were distributed along the upstream–downstream gradient of each river to sample the whole spatial structure of each metapopulation. For logistical reasons, some localities were not sampled each year, but an average of 8–9 localities was sampled each year per metapopulation. Sampling was done according to a standardized electrofishing protocol covering a 500–2000 m² surface section depending on the sampled locality. To ensure year-to-year comparisons, we did not vary the sampling surface at the locality level over time. All dace ($N_{\text{tot}} = 2264$) were anaesthetized, counted (to quantify dace abundance for each locality) and measured, and a piece of a pelvic fin was removed and stored in ethanol for each individual. All individuals were returned alive to their sampling locality. Permit numbers from regional authorities (i.e. the ‘Directions Départementales des Territoires’) are provided in Supplementary material Appendix 1 Table A1.

Laboratory analyses and genetic diversity assessment

We extracted the total DNA from fins following Aljanabi and Martinez (1997). Individual genotypes were obtained at twelve microsatellite loci (Supplementary material Appendix 1 Table A2). We estimated the frequencies of null alleles using the R package ‘PopGenReport’ (Adamack and Gruber 2014). We found a relatively high frequency of null alleles in one marker (Rhca20, Supplementary material Appendix 1 Table A3). Analyses were therefore run with and without this specific marker to ensure the reliability of results. Since there were no significant differences between the results obtained with and without Rhca20, we only present those with the twelve markers.

Genetic diversity was quantified using seven genetic indices. Five of them were calculated using the R package ‘adeget’ (Jombart 2008) at the marker level: the number of alleles (NA), the allelic richness (AR, i.e. the mean number of alleles across loci standardized for the lowest sampling size using a rarefaction procedure), the inbreeding coefficient (Fis), the expected heterozygosity (He) and the observed heterozygosity (Ho). We also estimated the M-ratio (Garza and Williamson 2001) because this index efficiently captures the signatures of recent genetic bottlenecks in spatially structured populations potentially experiencing downstream-biased asymmetric gene flow, such as riverine populations (Paz-Vinas et al. 2013). The M-ratio detects

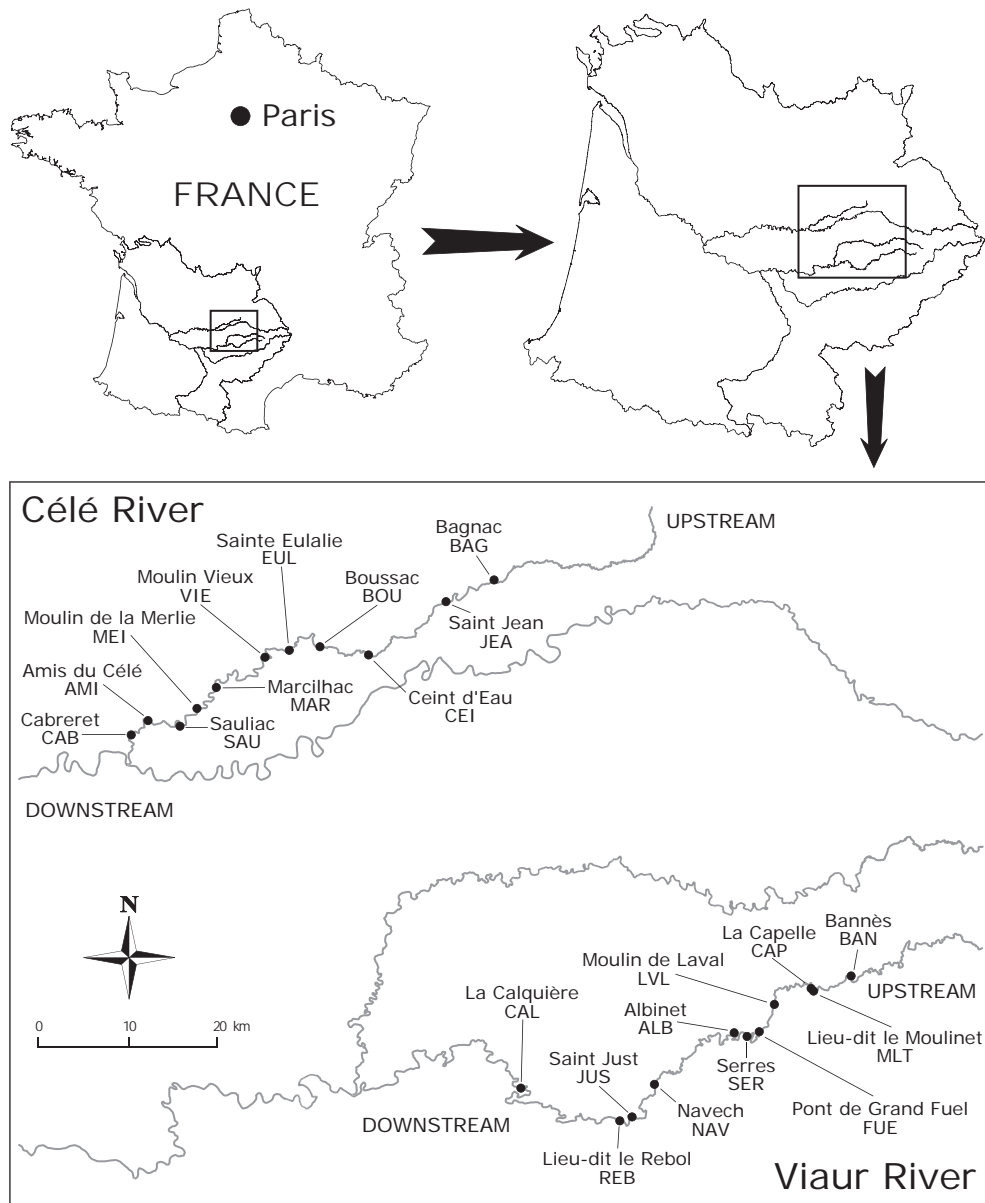


Figure 1. Maps of the Viaur and Célé Rivers, together with the different sampling localities (11 per river) and their distribution along the upstream–downstream gradient of each river.

genetic bottlenecks via a loss of alleles relative to the allelic range, the latter of which is supposed to decrease slower than the number of alleles during a demographic collapse (Garza and Williamson 2001). Empirical M -ratio values that were lower than a critical value of 0.68 indicate significant bottlenecks (Garza and Williamson 2001). The M -ratio was calculated at the marker level using a customized R script (Mathieu-Bégné et al. 2018). Finally, we also estimated the effective metapopulation size (N_e) for each year and each metapopulation using the linkage disequilibrium method implemented in the software NeEstimator V2.01 (Do et al. 2014) and a sliding window of three years corresponding to the generation time of dace (Skrbinšek et al. 2012).

Statistical analyses

Temporal demographic trends and impact of the spatial structure of metapopulation

We computed a generalized linear mixed model (GLMM) to test whether there were significant temporal trends in dace abundance and whether these trends varied between the two metapopulations. Since the response variable was the number of dace caught per year and per locality, a Poisson error term distribution was fitted. Explanatory variables (fixed effects) were metapopulation identity (i.e. the Viaur or Célé River), sampling year and the resulting two-term interaction. Locality identity was included as an intercept-only random variable.

We further investigated whether temporal demographic changes were homogeneously distributed across each metapopulation by testing the relationship between temporal demographic changes measured at the locality level and the spatial position of each locality along the upstream–downstream gradient of each metapopulation. We specifically used an additive linear model that assumed a Gaussian error term distribution, the distance from the river source of each locality and metapopulation identity as explanatory variables, and the strength of the temporal trend at the locality level (i.e. the slope of the relationship between dace abundance and year of sampling) as the response variable.

Population dynamics models and processes underlying temporal demographic trends

We aimed at evaluating, for each metapopulation, whether demographic changes observed over time resulted from changes in the intrinsic growth rate (IGR) and/or in the strength of density-dependence processes. To do so, we fitted hierarchical N-mixture models (Hostetler and Chandler 2015) to the abundances recorded across localities in each metapopulation, in order to estimate the two parameters cited above for each metapopulation and for each sampling year. These models are a class of state–space models integrating 1) a sampling process relating the observed abundances (denoted N , i.e. the number of individuals detected during a sampling event) to the true abundances (denoted X , i.e. the actual number of individuals present during a sampling event) and 2) a population dynamics process that describes the evolution of abundances through time (De Valpine and Hastings 2002). The observation process was described by a binomial distribution:

$$X_{i,t} \sim \text{Bin}(N_{i,t}, p_i)$$

where p_i is the probability of detection at locality i . To model dace abundances at locality i and time t , we used a Poisson distribution:

$$N_{i,t} \sim \text{Pois}(E(N_{i,t}))$$

where $E(N_{i,t})$ is the expected dace abundance at locality i and time t under a stock–recruitment Ricker model. On the log-scale the model is represented by:

$$\log(E(N_{i,t})) = \log(N_{i,t-1}) + \rho - \eta \times N_{i,t-1}$$

where ρ and η are fixed effects representing the intrinsic metapopulation growth rate (i.e. the rate of metapopulation increase when $N_{i,t-1}=0$) and the strength of density-dependence, respectively. Both parameters were assumed to follow normal distributions centred on 0 with large standard deviations. To allow for stochastic differences between localities in the IGR and for stochastic year effects common to all localities, we introduced the parameters S_i and T_t to the

model described above, representing the random locality and random year effects, respectively. S_i and T_t were assumed to follow normal distributions centred on 0, with standard deviations σ_S and σ_T representing the magnitude of the variability among localities and years, respectively. Half-Cauchy distributions were used as priors for σ_S and σ_T (Gelman 2006). Finally, the priors for the initial values N_1 of each time series were Poisson distributions with means equal to the average number of individuals captured during the survey, increased by one (Kéry and Schaub 2012). To obtain posterior distributions of parameters (Clark and Bjørnstad 2004), we adopted a Bayesian approach using JAGS 3.3.0 (Plummer 2003) run through the R package ‘R2jags’ (Su and Yajima 2012). Convergence was visually assessed and confirmed using the Gelman and Rubin statistic for all parameters (Gelman and Rubin 1992), and highest posterior density (HPD) intervals were used as 95% credible intervals.

Temporal genetic diversity trends

We computed independent GLMMs or GLMs to test the effect of temporal trends on each genetic index (i.e. NA, AR, Fis, Ho, He, M-ratio and Ne used as response variables). Gaussian error term distributions were assumed for all indices but NA and Ne, for which a Poisson error term distribution and a Quasi-Poisson error term distribution (to deal with overdispersion) were assumed, respectively. Metapopulation identity, sampling year and the resulting two-term interaction were set as fixed effects. The marker identity was set as a random intercept for each genetic index except for Ne, for which we used a simple GLM (because Ne was not calculated at the marker level). Additionally, we tested whether rare alleles were more likely to be lost (rather than common alleles) in the Viaur metapopulation, as expected theoretically in declining populations (Nei et al. 1975). To do so, we used a Wilcoxon rank-sum test comparing for the Viaur metapopulation 1) the allele frequencies measured across the first four years of the study (2005–2008, i.e. before the population collapse) for alleles that are still present in the four last years of the survey (2011–2014, i.e. after the population collapse) to 2) allele frequencies measured across 2005–2008 for alleles that have been lost in the last four years of the survey. Finally, we plotted direct relationships between temporal demographic and genetic diversity variations for each genetic diversity index, and tested their relationships using Mantel correlation tests conducted for each metapopulation independently (i.e. resulting in twelve Mantel tests). The significance of each Mantel test was evaluated using Spearman correlation coefficients and 1000 permutations. Mantel tests were performed using the R package ‘vegan’ (Oksanen et al. 2011).

The impact of metapopulation spatial structure on temporal trends of genetic diversity

To investigate the impact of the metapopulation spatial structure on genetic diversity trends, we first tested the spatial distribution of the ‘initial’ genetic diversity (i.e. the

genetic diversity observed for the first year of the survey) using GLMs that assumed Gaussian error term distributions. Initial genetic diversity was computed for NA, Fis, He, Ho and the M-ratio at each locality for the first monitoring year (2005 for the Viaur River metapopulation and 2006 for the Célé River metapopulation) and used as response variables in separated models. The explanatory variables were metapopulation identity and the distance from the source of each locality.

Second, we evaluated the marginal impact of each local population on changes in temporal genetic diversity in the declining metapopulation. To do so, we re-ran the analyses in order to test for temporal trends in the genetic diversity presented above, but by iteratively removing data from one locality from the whole dataset (from the most upstream locality to the most downstream locality, i.e. localities were not randomly removed). For each combination (all localities sampled in each year minus one being excluded) we calculated genetic indices for each year at the marker level and used GLMMs with the marker as a random effect as described above to estimate the slopes of the relationships between genetic diversity indices and the year of sampling, together with its standard error. We excluded Ne from this analysis to allow robust models with information at the marker level. We finally compared these slope estimates to the estimate calculated when all localities are included in the analyses. If the removal of one specific locality leads to a slope estimate steeper than the slope estimated from the whole dataset, one can consider that the population in this specific locality may serve as a genetic reservoir (and potentially as a source) in the metapopulation, since this local population actually provides some marginal genetic diversity to the metapopulation, hence dampening the expected genetic diversity loss.

All statistical analyses were done using the R software (ver. 3.4.2 <www.r-project.org>), and all GLMMs were fitted using the package 'glmmADMB' (Bolker et al. 2012).

Data deposition

Raw data and scripts required for statistical analyses are available at <<https://doi.org/10.6084/m9.figshare.5999171>>.

Results

Temporal demographic trends and impact of the spatial structure of metapopulations

As expected, we found that demographic trends over time significantly varied between the two metapopulations (Table 1a). Dace displayed a slight but significant increase in metapopulation size over time in the Célé River, whereas dace abundance severely declined in the Viaur River (Fig. 2a). We further detected a positive relationship between the magnitude of the demographic changes measured at the local population level and their distance from the river source in both metapopulations ($F = 5.916$, $df = 1,15$, $p\text{-value} = 0.029$,

Table 1. Output of GLMMs (a–f) and GLM (h) testing the effect of metapopulation identity, year, and the resulting interaction (included only when significant) on (a) dace abundance, (b) allelic richness, (c) expected heterozygosity, (d) observed heterozygosity, (e) number of alleles, (f) Fis, (g) M-ratio and (h) effective population size.

	df ^a	Statistic ^b	p-value
a) Number of dace ^c			
Year	1,156	56.333	< 0.001
Metapopulation	1,156	177.34	< 0.001
Year: metapopulation	1,156	171.875	< 0.001
b) Allelic richness ^b			
Year	1,223	0.098	0.754
Metapopulation	1,223	256.637	< 0.001
c) Expected heterozygosity ^b			
Year	1,223	0.786	0.376
Metapopulation	1,223	65.885	< 0.001
d) Observed heterozygosity ^b			
Year	1,223	0.837	0.361
Metapopulation	1,223	35.224	< 0.001
e) Number of alleles ^c			
Year	1,223	3.185	0.074
Metapopulation	1,223	16.694	< 0.001
Year: metapopulation	1,223	14.693	< 0.001
f) Fis ^b			
Year	1,222	4.187	0.042
Metapopulation	1,222	6.471	0.012
Year: metapopulation	1,222	6.473	0.012
g) M-ratio ^b			
Year	1,222	1.157	0.283
Metapopulation	1,222	7.921	0.005
Year: metapopulation	1,222	8.014	0.005
h) Effective population size ^b			
Year	1,15	141.270	< 0.001
Metapopulation	1,15	263.639	< 0.001
Year: Metapopulation	1,15	15.817	< 0.001

^aDegrees of freedom at the numerator and denominator, respectively.

^bStatistics used in these models are Fisher statistics.

^cStatistics used in these models are χ^2 -statistics.

Fig. 2b). This correlation indicated that demographic declines in the Viaur metapopulation were stronger in upstream sites than in downstream sites (where the most downstream local population was actually demographically stable, Fig. 2b) and that demographic increases in the Célé metapopulation were stronger in downstream sites than in upstream sites.

Population dynamics models and processes underlying temporal demographic trends

In support of previous demographic temporal trend analyses, we found a positive IGR with HPD intervals that did not overlap zero for dace from the Célé River, whereas a negative IGR was measured for dace from the Viaur River, although the HPD intervals overlapped zero (Fig. 3a). Our metapopulation dynamics models further revealed significant regulation through density-dependence processes for the Célé River metapopulation (positive value of η), whereas a slight negative value of η was found for the Viaur River metapopulation (Fig. 3b). In both metapopulations, we found strong year-to-year variations in the IGR. More specifically,

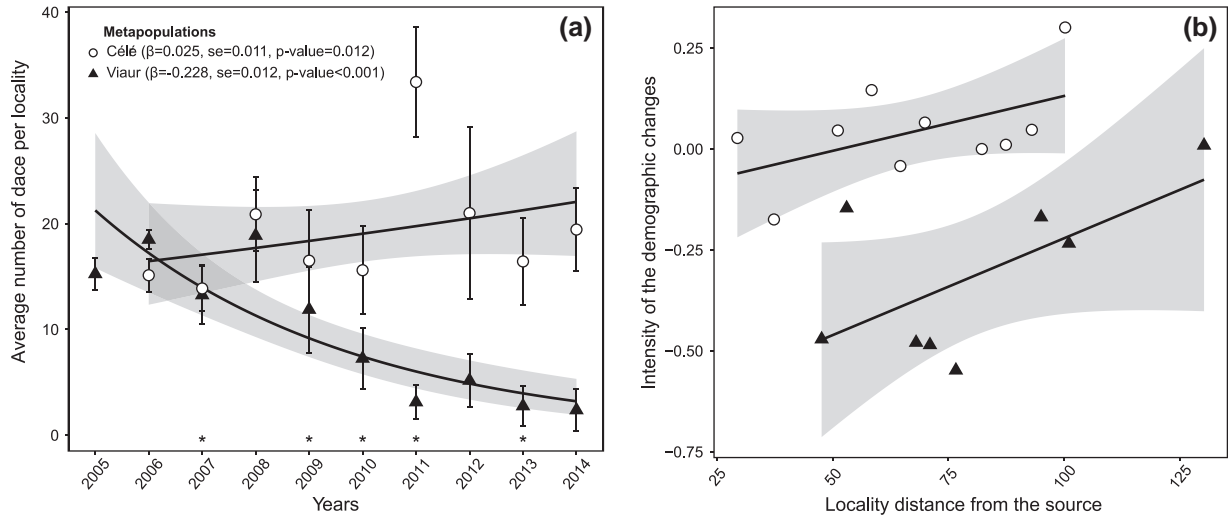


Figure 2. (a) Temporal changes in dace *Leuciscus burdigalensis* abundances in the Viaur and Célé metapopulations. Error bars are standard deviation. Grey areas are confidence intervals of the prediction (lines) from a linear model. Stars represent years for which intrinsic growth rates are significantly negative. (b) Relationship between the strength of the demographic changes (i.e. the slope of the relationship between dace abundance and years) for each local population and the distance from the source of their respective locality. Grey areas are confidence intervals of the prediction (lines) from models.

IGR values were always positive for the Célé River metapopulation, with HPD intervals that never overlapped zero (Fig. 3c). In contrast, IGR values were negative for most years for the Viaur River metapopulation, with five years specifically showing significant negative IGR values (2007, 2009–2011, 2013, Fig. 3c).

Temporal genetic diversity trends

He, Ho and AR were, on average, 7–26% lower for the Viaur River metapopulation than from the Célé River metapopulation (Table 1b–d, Supplementary material Appendix 1 Fig. A1), although we did not detect any significant temporal trends for these genetic indices (Table 1b–d). In contrast, significant interaction terms between ‘metapopulation identity’ and ‘sampling year’ were detected for NA, Fis and the M-ratio (Table 1e–g), indicating that temporal trends vary between metapopulations for these three genetic parameters. For both NA and M-ratio, we detected a strong and significant decrease over time in the Viaur River metapopulation, whereas these two genetic parameters were stable over time in the Célé River metapopulation (Fig. 4a–b). Interestingly, the values observed for the M-ratio for the Viaur River metapopulation were always lower than 0.68 (Fig. 4b). Fis significantly increased over time in the Viaur River metapopulation, whereas it significantly decreased in the Célé River metapopulation (Fig. 4c). Temporal trends in Ne estimated from genetic markers to lesser extent mirrored the temporal trends in dace abundance highlighted from demographic data: Ne increased sharply and significantly over time in the Célé River metapopulation, whereas Ne remained very low and stable over time in the Viaur River metapopulation (Table 1h, Fig. 4d). Ne values estimated for the Viaur River metapopulation never exceeded ~50 individuals and

were always smaller than values estimated in the Célé River metapopulation (Table 1h, Fig. 4d).

Furthermore, alleles that were lost in the last four years had lower initial frequencies than alleles that were still present in the last four years, indicating that, as expected, rare alleles were first lost during the decline ($W = 5237$, $p\text{-value} < 0.001$, Supplementary material Appendix 1 Fig. A2). Finally, the observed relationship between temporal demographic and genetic variations for NA and the M-ratio also supports that the demographic decline observed in the Viaur metapopulation is associated with genetic diversity loss (Supplementary material Appendix 1 Fig. A3). Notably, we identified significant relationships between temporal demographic and genetic variations, implying both NA and the M-ratio in the Viaur metapopulation, and a significant relationship between temporal demographic and genetic variations for NA in the Célé metapopulation (Supplementary material Appendix 1 Table A4).

The impact of metapopulation spatial structure on temporal trends of genetic diversity

We found that initial genetic diversity was spatially structured for two indices (NA and AR). We indeed highlighted a positive trend between these two indices and the distance from the source of each locality ($F_{NA} = 6.023$, $df_{NA} = 1,12$, $p\text{-value}_{NA} = 0.030$, $F_{AR} = 5.246$, $df_{AR} = 1,12$, $p\text{-value}_{AR} = 0.041$, Fig. 5), indicating that genetic diversity tended, as expected, to be higher downstream.

Regarding the impact of metapopulation spatial structure on temporal trends of genetic diversity, we found that the dace population from one locality of the Viaur River metapopulation (‘La Calquière’, localized in the most downstream part of the river, Fig. 1) had a marginal impact on the loss

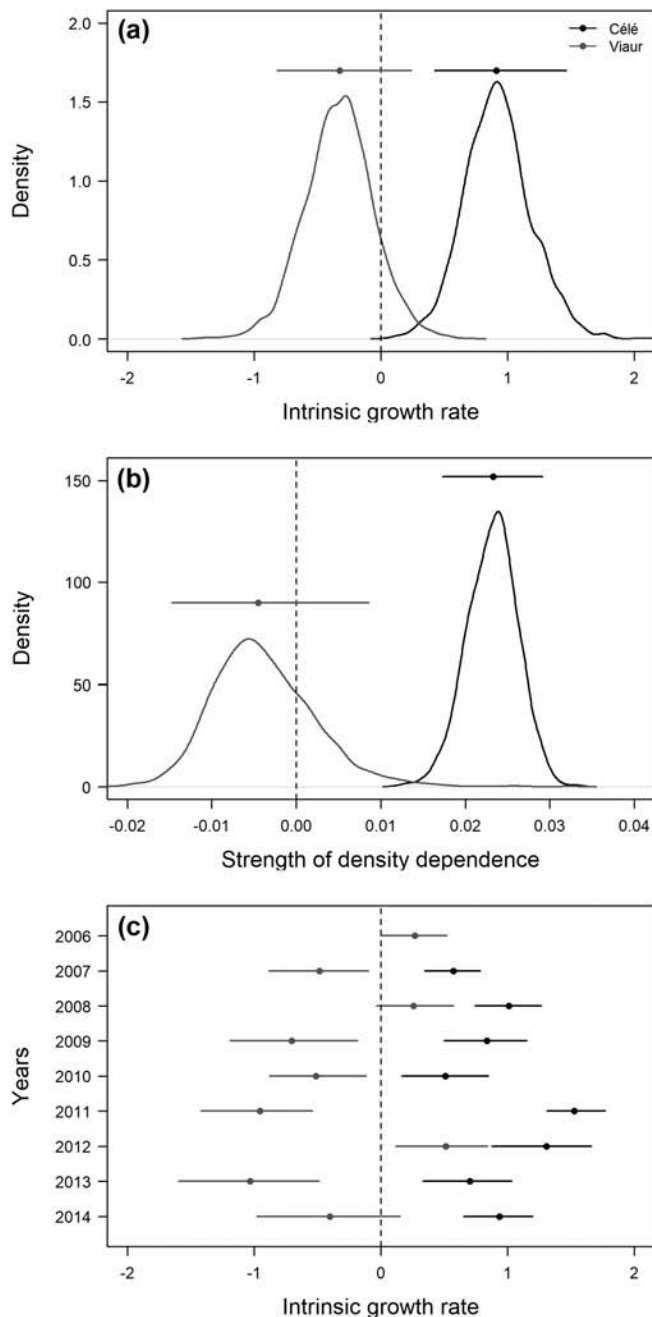


Figure 3. Posterior distributions of (a) the intrinsic growth rate (IGR), (b) the strength of density dependence and (c) temporal variations in IGR. The latter was obtained by adding random sampling sites and years effects to the fixed value of IGR. In (a) and (b), the curves represent the posterior density distribution of the parameters for both metapopulations. In the three panels, the horizontal lines represent the 95% of the highest posterior density (HPD) intervals whereas the points represent the median of the posterior distribution and the vertical dashed line is indicative of the zero value. HPD intervals that do not overlap this line represent significant effects.

of genetic diversity measured over time for several indices. More precisely, when this local population was removed from the whole dataset, steeper slope estimates (compared to the

estimates based on the whole dataset) were detected for the relationship between NA and year of sampling (Fig. 6a) for the relationship between Fis and year of sampling (Fig. 6e) and for the relationship between He and year of sampling (Fig. 6f). These results suggest that this most downstream local population likely acts as a genetic diversity reservoir in the Viaur River metapopulation.

Discussion

We confirmed the incidence of a severe demographic decline during the monitoring period in the dace metapopulation from the Viaur River, corresponding to an ~80% abundance decrease that occurred in less than ten years. Meanwhile, dace abundance increased over time in the Célé River metapopulation. We further show that the intrinsic growth rates of dace metapopulations were mostly negative in the Viaur River, whereas they were always positive in the Célé River, thus confirming the contrasting demographic trends observed for these two and supporting an expected decline of genetic diversity in the Viaur metapopulation (Reed et al. 2007, Hostetler et al. 2013). Second, our study highlights that the demographic decline observed in the Viaur River was not homogeneous among local populations. We specifically demonstrate that the most downstream local dace population sampled in this riverscape was actually stable over time (a tendency also observed in the Célé River Fig. 2b). This finding is in line with the general idea that upstream populations are more prone to local extinctions than downstream populations in riverine networks (Gotelli and Taylor 1999, Fagan 2002, Mari et al. 2014).

At the genetic level, our longitudinal survey revealed that, contrary to the stable Célé River metapopulation, the collapsing metapopulation was suffering a genetic bottleneck, as it was experiencing a loss of genetic diversity and an increase of its inbreeding coefficient (generally associated with higher extinction risk, Frankham 1995). This global loss of genetic diversity in the Viaur River metapopulation seems to be intrinsically associated with the demographic collapse we identified as documented by Spielman et al. (2004). For instance, the decrease in the number of observed alleles is directly linked to the loss of individuals observed in many localities of the Viaur River. We indeed found that rare alleles were more prone to disappear from the Viaur metapopulation compared to common alleles, as it is expected in collapsing populations (Nei et al. 1975), and we can therefore assume that these alleles will only be recovered if individuals from peripheral populations immigrate (Chen et al. 2016). We further found that the inbreeding coefficient decreased over time in the Célé River metapopulation, which indicates that this metapopulation became closer to the Hardy–Weinberg equilibrium. This may be attributed to the significant increase in dace abundance detected in this metapopulation, and shows that a slight increase in metapopulation abundance may help reduce inbreeding in wild

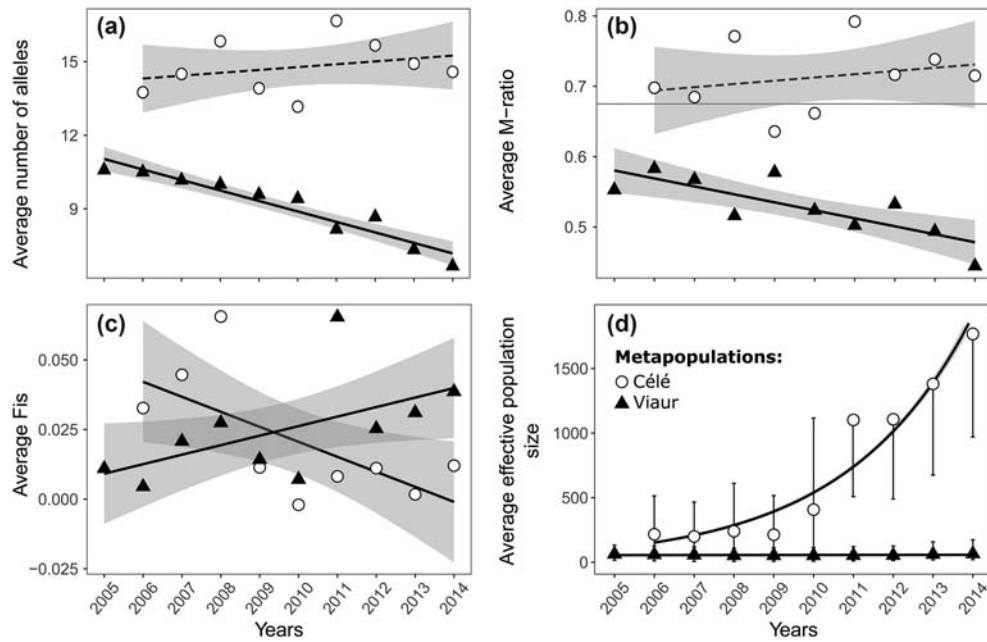


Figure 4. Temporal changes in (a) mean number of alleles, (b) mean M-ratios, with the grey horizontal line that displays the significant limit of 0.68 (Garza and Williamson 2001), (c) mean Fis, and (d) Ne for dace from the Viaur and Céle metapopulations. Note that for Ne estimates, when no upper error bars are displayed this indicates infinite estimates of the upper limit. Grey areas are confidence intervals of the predictions (lines) from a linear model. Solid lines are significant, whereas dashed lines are non-significant.

metapopulations. In contrast, departure from the Hardy–Weinberg equilibrium was stronger over time in the declining metapopulation, which probably reflects the higher risk of inbreeding due to the extremely low and declining number of effective breeders measured in this metapopulation

and likely resulting in the negative intrinsic growth rate we identified (Waples 2002, Reed et al. 2007).

Interestingly, not all genetic diversity indices co-varied with this demographic decline, as we failed to detect temporal changes for heterozygosity and allelic richness. This

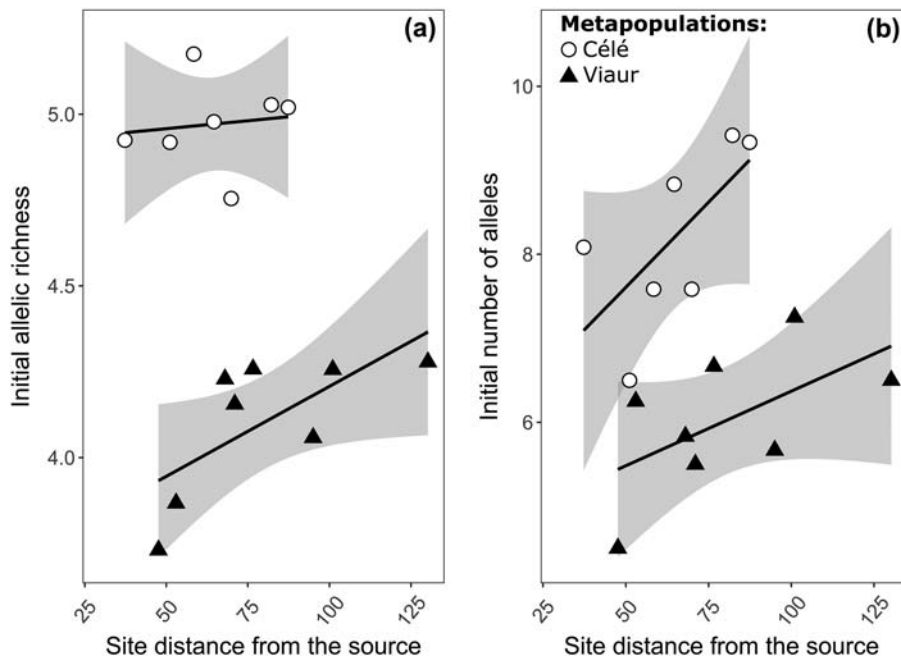


Figure 5. Relationship between the initial genetic diversity measured as the allelic richness (a) and the number of alleles (b) in each local population and the distance from the source of each locality. Grey areas are confidence intervals of the predictions (lines) from linear models.

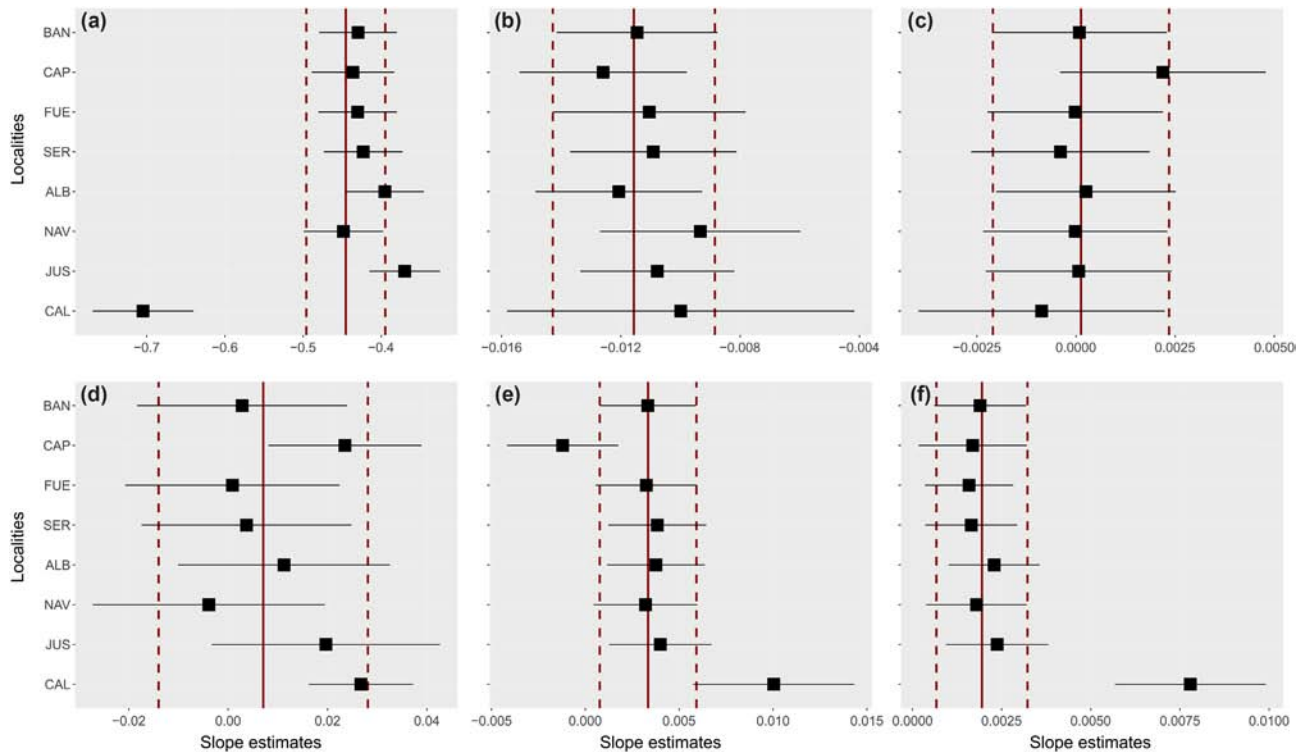


Figure 6. Forest plots for the number of alleles (a), the M-ratio (b), the observed heterozygosity (c), the allelic richness (d), the F_{IS} (e) and the expected heterozygosity (f) slope estimates for the relationship between each of these indices and the year of sampling, in the Viaur metapopulation. Each local population names (BAN, CAP, FUE, SER, ALB, NAV, JUS and CAL, ranked from upstream to downstream) refers to the dataset used to estimate slopes (i.e. the whole dataset minus the named local population). Note that only the sites that were sampled in all years were considered in this analysis. Red vertical line refers to the observed estimate for the whole dataset and dashed lines refer to the confident interval of this estimate.

probably reflects the differential sensitivity of genetic indices to demographic declines, which was recently demonstrated theoretically (Hoban et al. 2014). Some indices could be characterized by non-linear temporal changes that may be detectable only once a threshold is reached (Scheffer et al. 2001), which may require a longer time series to be attained (Antao et al. 2011). In any cases, genetic diversity was globally lower in the Viaur than in the C  l   metapopulation and both effective metapopulation sizes and the M-ratio were extremely low in the Viaur metapopulation, even before the beginning of the demographic decline.

Finally, we exemplified how metapopulation structure could dampen the loss of genetic diversity at the metapopulation scale, notably through source local populations, such as the one sampled at the most downstream locality ('La Calqui  re') in the Viaur River. We notably found that if this local population would not have sustained large dace abundances over time (i.e. would have critically declined instead of being stable, as we actually observed) the decrease in the number of alleles at the metapopulation scale would have been much steeper over this 10-year period. Similarly, this local population also contributed to limit deviation from the Hardy-Weinberg equilibrium and reduced the bottleneck signal observed at the metapopulation scale. Indeed, without this local population, we would have recorded increasing

expected heterozygosity over time, together with a constant number of heterozygotes (measured by Hobs, Fig. 6c, f), which is generally interpreted as a signal of bottleneck (Luikart and Cornuet 1998). This downstream local population was both the most stable demographically and the most diverse genetically, hence contributing to the explanation of its marginal influence at the metapopulation scale. This demonstrates that the spatial variation between demographic parameters and genetic parameters observed in certain metapopulations (such as those living in riverscapes) may dampen the temporal variation observed at the metapopulation scale ('portfolio effect', Doak et al. 1998, Anderson et al. 2013). However, the high level of fragmentation by dams and weirs in the Viaur River might limit potential genetic and demographic rescue effects provided by emigration from downstream localities to upstream localities (Chen et al. 2016). Thus, any genetic and demographic rescue effect in the Viaur River would be only possible through human-assisted migration.

It is worth noting that in this study the two metapopulations were analyzed from a linear perspective, i.e. along the upstream-downstream gradient of the main stem. In stream metapopulations, however, we can expect specific demographic and genetic dynamics arising from the dendritic structure of the network (Paz-Vinas et al. 2015, Morrissey and de Kerckhove 2009). For instance, tributaries can in some

cases serve as genetic reservoirs that sustain the entire genetic diversity observed downstream through ‘genetic mass effects’ (Kunin 1998, Campbell Grant et al. 2007, also known as ‘downstream-biased gene flow’, Paz-Vinas et al. 2015). This is nonetheless unlikely in our case study since dace (in the two sub-river basins considered in this study) mainly live the main stem and rarely use tributaries as main habitats (because they are generally too cold and too steep for dace). In both the Célé and Viaur metapopulations, higher levels of genetic diversity observed downstream are hence more likely to be the produce of a past upstream-directed colonization process or of higher effective population sizes downstream rather than from mass effects from upstream to downstream (as observed in many river systems for many organisms, Paz-Vinas et al. 2015). We hence reasonably assume that the demographic and genetic dynamics observed in the most downstream locality of the Viaur River likely reflect a ‘reservoir’ in this area, rather than a sink resulting from a ‘mass effect’. Nonetheless, we argue that further long-term demo-genetic monitoring should be conducted in dendritic river networks to better understand the role of spatial structures in shaping the demographic and genetic stability of the metapopulations inhabiting these specific ecosystems (Anderson et al. 2013).

To conclude, our study demonstrates, in a continuous real-time demo-genetic design, that a demographic decline of a wild metapopulation can be associated with a significant loss in genetic diversity over a period as short as ten years. This shows the usefulness of continuous real-time monitoring to quantify, at a fine time-scale, both the genetic and demographic changes occurring in declining populations, which has strong implications for the prediction and prevention of extinction vortices in the wild. Continuous real-time monitoring combining genetic and demographic indicators is still rarely used (Habel et al. 2014), but we demonstrate that these indicators can jointly vary over short time scales. Moreover, we demonstrate how the spatial arrangement and the specificity of local populations within a landscape can modulate both local extinction rates and local genetic diversity distributions, which may dampen the pervasive genetic effects of demographic declines at the metapopulation scale. We call for more integrated monitoring programmes, because they can realistically inform both the ecological and evolutionary viability of endangered metapopulations.

Acknowledgements – We thank all the colleagues that helped with sampling. This work was performed using HPC resources from CALMIP (allocation P1003). This work has been done in two research units (SETE & EDB) that are part of the ‘Laboratoire d’Excellence’ (LABEX) entitled TULIP (ANR-10-LABX-41). This work is part of the project INCLIMPAR (ANR-11-JSV7-0010) supported by a grant from the ‘Agence Nationale de la Recherche’.

Author contributions – GL and SB coordinated the study, organized the long-term surveys and performed the molecular analyses. EMB, SB, IPV and MC ran statistical analyses. EMB, SB, GL, IPV and MC wrote the manuscript. All authors agreed to be held accountable for the content therein and approved the final version of the manuscript.

Ethical statement – Permit numbers required to capture and manipulate fish are provided in Supplementary material Appendix 1 Table A1. These permits are in accordance with current ethical laws in France.

Conflict of interest – We have no competing interest.

References

- Adamack, A. T. and Gruber, B. 2014. Popgenreport: simplifying basic population genetic analyses in R. – *Methods Ecol. Evol.* 5: 384–387.
- Aljanabi, S. and Martinez, I. 1997. Universal and rapid salt-extraction of high quality genomic DNA for PCR-based techniques. – *Nucleic Acids Res.* 25: 4692–4693.
- Altermatt, F. 2013. Diversity in riverine metacommunities: a network perspective. – *Aquat. Ecol.* 47: 365–377.
- Anderson, S. C. et al. 2013. Ecological prophets: quantifying metapopulation portfolio effects. – *Methods Ecol. Evol.* 4: 971–981.
- Antao, T. et al. 2011. Early detection of population declines: high power of genetic monitoring using effective population size estimators. – *Evol Appl.* 4: 144–154.
- Barson, N. J. et al. 2009. Population genetic analysis of microsatellite variation of guppies (*Poecilia reticulata*) in Trinidad and Tobago: evidence for a dynamic source–sink metapopulation structure, founder events and population bottlenecks. – *J. Evol. Biol.* 22: 485–497.
- Bolker, B. et al. 2012. Getting started with the glmmADMB. – R package ver. 3.4.3 <<http://glmmadmb.r-forge.r-project.org>>.
- Campbell Grant, E. H. et al. 2007. Living in the branches: population dynamics and ecological processes in dendritic networks. – *Ecol. Lett.* 10: 165–175.
- Cappuccino, N. and Price, P. W. 1995. Population dynamics: new approaches and synthesis. – Elsevier.
- Carlson, S. M. et al. 2014. Evolutionary rescue in a changing world. – *Trends Ecol. Evol.* 29: 521–530.
- Chen, N. et al. 2016. Genomic consequences of population decline in the endangered Florida scrub-jay. – *Curr. Biol.* 26: 2974–2979.
- Clark, J. and Bjørnstad, O. 2004. Population time series: process variability, observation errors, missing values, lags, and hidden states. – *Ecology* 85: 3140–3150.
- De Valpine, P. and Hastings, A. 2002. Fitting population models incorporating process noise and observation error. – *Ecol. Monogr.* 72: 57–76.
- Devillard, S. et al. 2011. Linking genetic diversity and temporal fluctuations in population abundance of the introduced feral cat (*Felis silvestris catus*) on the Kerguelen archipelago. – *Mol. Ecol.* 20: 5141–5153.
- Do, C. et al. 2014. NeEstimator: re-implementation of software for the estimation of contemporary effective population size from genetic data. – *Mol. Ecol. Resour.* 14: 209–214.
- Doak, D. F. et al. 1998. The statistical inevitability of stability–diversity relationships in community ecology. – *Am. Nat.* 151: 264–276.
- Dunning, J. B. et al. 1992. Ecological processes that affect populations in complex landscapes. – *Oikos* 65: 169–175.
- Fagan, W. F. 2002. Connectivity, fragmentation, and extinction risk in dendritic metapopulations. – *Ecology* 83: 3243–3249.
- Frankham, R. 1995. Inbreeding and extinction: a threshold effect. – *Conserv. Biol.* 9: 792–799.

- Fronhofer, E. A. and Altermatt, F. 2017. Classical metapopulation dynamics and eco-evolutionary feedbacks in dendritic networks. – *Ecography* 40: 1455–1466.
- Gaggiotti, O. E. 1996. Population genetic models of source–sink metapopulations. – *Theor. Popul. Biol.* 50: 178–208.
- Garza, J. C. and Williamson, E. G. 2001. Detection of reduction in population size using data from microsatellite loci. – *Mol. Ecol.* 10: 305–318.
- Gelman, A. 2006. Prior distributions for variance parameters in hierarchical models. – *Bayesian Anal.* 1: 515–534.
- Gelman, A. and Rubin, D. 1992. Inference from iterative simulation using multiple sequences. – *Stat. Sci.* 7: 457–511.
- Gotelli, N. J. and Taylor, C. M. 1999. Testing macroecology models with stream-fish assemblages. – *Evol. Ecol. Res.* 1: 847–858.
- Habel, J. C. et al. 2014. The relevance of time series in molecular ecology and conservation biology: temporal comparison of genetic data. – *Biol. Rev.* 89: 484–492.
- Hanski, I. 1998. Metapopulation dynamics. – *Nature* 396: 41–49.
- Hansson, B. et al. 2000. Increase of genetic variation over time in a recently founded population of great reed warblers (*Acrocephalus arundinaceus*) revealed by microsatellites and DNA fingerprinting. – *Mol. Ecol.* 9: 1529–1538.
- Hildner, K. K. et al. 2003. The relationship between genetic variability and growth rate among populations of the pocket gopher, *Thomomys bottae*. – *Conserv. Genet.* 4: 233–240.
- Hoban, S. et al. 2014. Comparative evaluation of potential indicators and temporal sampling protocols for monitoring genetic erosion. – *Evol. Appl.* 7: 984–998.
- Hostetler, J. A. and Chandler, R. B. 2015. Improved state–space models for inference about spatial and temporal variation in abundance from count data. – *Ecology* 96: 1713–1723.
- Hostetler, J. A. et al. 2013. A cat’s tale: the impact of genetic restoration on Florida panther population dynamics and persistence. – *J. Anim. Ecol.* 82: 608–620.
- Jangjoo, M. et al. 2016. Connectivity rescues genetic diversity after a demographic bottleneck in a butterfly population network. – *Proc. Natl Acad. Sci. USA* 113: 10914–10919.
- Jombart, T. 2008. adegenet: a R package for the multivariate analysis of genetic markers. – *Bioinformatics* 24: 1403–1405.
- Kaeuffer, R. et al. 2007. Unexpected heterozygosity in an island mouflon population founded by a single pair of individuals. – *Proc. R. Soc. B* 274: 527–533.
- Keith, P. et al. 2011. Les poissons d’eau douce de France. – Biotope.
- Kéry, M. and Schaub, M. 2012. Bayesian population analysis using WinBUGS: a hierarchical perspective. – Academic Press.
- Kunin, W. E. 1998. Biodiversity at the edge: a test of the importance of spatial ‘mass effects’ in the Rothamsted Park grass experiments. – *Proc. Natl Acad. Sci. USA* 95: 207–212.
- Labonne, J. et al. 2008. Linking dendritic network structures to population demogenetics: the downside of connectivity. – *Oikos* 117: 1479–1490.
- Luikart, G. and Cornuet, J.-M. 1998. Empirical evaluation of a test for identifying recently bottlenecked populations from allele frequency data. – *Conserv. Biol.* 12: 228–237.
- Mari, L. et al. 2014. Metapopulation persistence and species spread in river networks. – *Ecol. Lett.* 17: 426–434.
- Mathieu-Bégné, E. et al. 2018. Resources for ‘Demographic and genetic collapses in spatially-structured populations: insights from a long-term survey in wild fish metapopulations.’. – Figshare fileset <<https://doi.org/10.6084/m9.figshare.5999171>>.
- Morrissey, M. B. and de Kerckhove, D. T. 2009. The maintenance of genetic variation due to asymmetric gene flow in dendritic metapopulations. – *Am. Nat.* 174: 875–889.
- Naranjo, E. J. and Bodmer, R. E. 2007. Source–sink systems and conservation of hunted ungulates in the Lacandon Forest, Mexico. – *Biol. Conserv.* 138: 412–420.
- Nei, M. et al. 1975. The bottleneck effect and genetic variability in populations. – *Evolution* 29: 1–10.
- Oksanen, J. et al. 2011. vegan: Community Ecology Package. – R package ver. 1.17-2 <<http://CRAN.R-project.org/package=vegan>>.
- Palstra, F. P. and Ruzzante, D. E. 2011. Demographic and genetic factors shaping contemporary metapopulation effective size and its empirical estimation in salmonid fish. – *Heredity* 107: 444–455.
- Paz-Vinas, I. and Blanchet, S. 2015. Dendritic connectivity shapes spatial patterns of genetic diversity: a simulation-based study. – *J. Evol. Biol.* 28: 986–994.
- Paz-Vinas, I. et al. 2013. The demographic history of populations experiencing asymmetric gene flow: combining simulated and empirical data. – *Mol. Ecol.* 22: 3279–3291.
- Paz-Vinas, I. et al. 2015. Evolutionary processes driving spatial patterns of intraspecific genetic diversity in river ecosystems. – *Mol. Ecol.* 24: 4586–4604.
- Plummer, M. 2003. JAGS: a program for analysis of Bayesian graphical models using Gibbs sampling. – *Proc. 3rd Int. Workshop Distrib. Stat. Comput.* 124: 125.
- Potvin, D. A. et al. 2017. Genetic erosion and escalating extinction risk in frogs with increasing wildfire frequency. – *J. Appl. Ecol.* 54: 945–954.
- Reed, D. H. et al. 2007. Genetic quality of individuals impacts population dynamics. – *Anim. Conserv.* 10: 275–283.
- Scheffer, M. et al. 2001. Catastrophic shifts in ecosystems. – *Nature* 413: 591–596.
- Schwartz, M. et al. 2007. Genetic monitoring as a promising tool for conservation and management. – *Trends Ecol. Evol.* 22: 25–33.
- Skrbinšek, T. et al. 2012. Monitoring the effective population size of a brown bear (*Ursus arctos*) population using new single-sample approaches. – *Mol. Ecol.* 21: 862–875.
- Spielman, D. et al. 2004. Most species are not driven to extinction before genetic factors impact them. – *Proc. Natl Acad. Sci. USA* 101: 15261–15264.
- Su, Y.-S. and Yajima, M. 2012. R2jags: a package for running jags from R. – R package ver. 0.03-08 <<http://CRAN.R-project.org/package=R2jags>>.
- Vuilleumier, S. et al. 2010. Effects of colonization asymmetries on metapopulation persistence. – *Theor. Popul. Biol.* 78: 225–238.
- Waples, R. 2002. Population viability analysis. – In: Beissinger S. R. and McCullough, D. R. (eds), *Definition and estimation of effective population size in the conservation of endangered species*. Univ. of Chicago Press, pp. 147–168.

Supplementary material (available online as Appendix oik-05511 at <www.oikosjournal.org/appendix/oik-05511>). Appendix 1.